Supporting Information for

Molecular Targeting of Immunosuppressants Using a Bifunctional Elastin-Like Polypeptide

Yaping Ju[†‡], Hao Guo[†], Frances Yarber[‡], Maria C. Edman[‡], Santosh Peddi[†], Srikanth Reddy Janga [‡],

J. Andrew MacKay[†, ‡, §*], and Sarah F. Hamm-Alvarez [†, ‡*]

†Department of Pharmacology and Pharmaceutical Sciences, School of Pharmacy, University of Southern California, Los Angeles, California 90089, United States
‡Department of Ophthalmology, USC Roski Eye Institute, Keck School of Medicine, University of Southern California, Los Angeles, California 90089, United States
§Department of Biomedical Engineering, Viterbi School of Engineering, University of Southern California, Los Angeles, California 90089, United States

*Co-corresponding authors

Address correspondence to:
Sarah F. Hamm-Alvarez, Ph. D.
Department of Ophthalmology
1450 San Pablo St, Room 4900, Mail Code #6103
USC Keck School of Medicine
Los Angeles, CA 90033
shalvar@med.usc.edu

J. Andrew MacKay, Ph. D.
Department of Pharmacology and Pharmaceutical Sciences
USC School of Pharmacy
1985 Zonal Avenue
Los Angeles CA 90033
jamackay@usc.edu

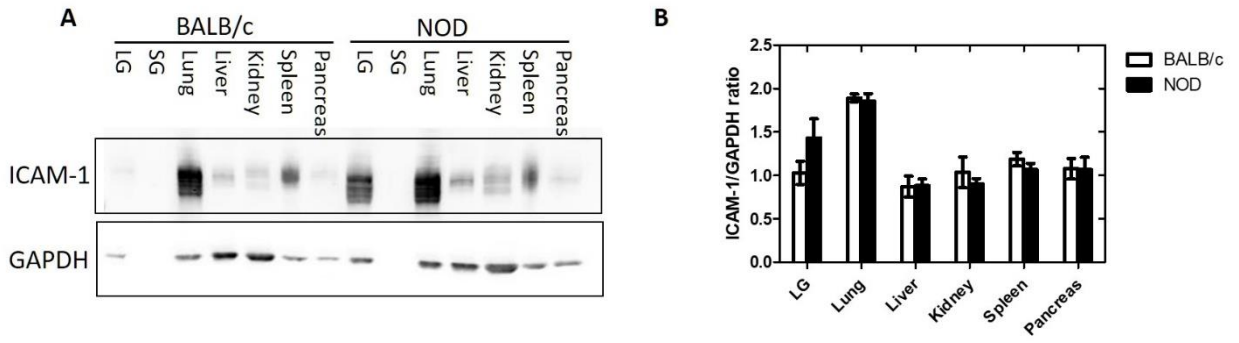

Figure S1. Protein levels of ICAM-1 in different tissues from BALB/c and NOD mice. A) A representative Western blot of ICAM-1 in different tissues from BALB/c and NOD mice. B) Quantification of ICAM-1 level normalized to GAPDH in different tissues of BALB/c and NOD mice (n=3).

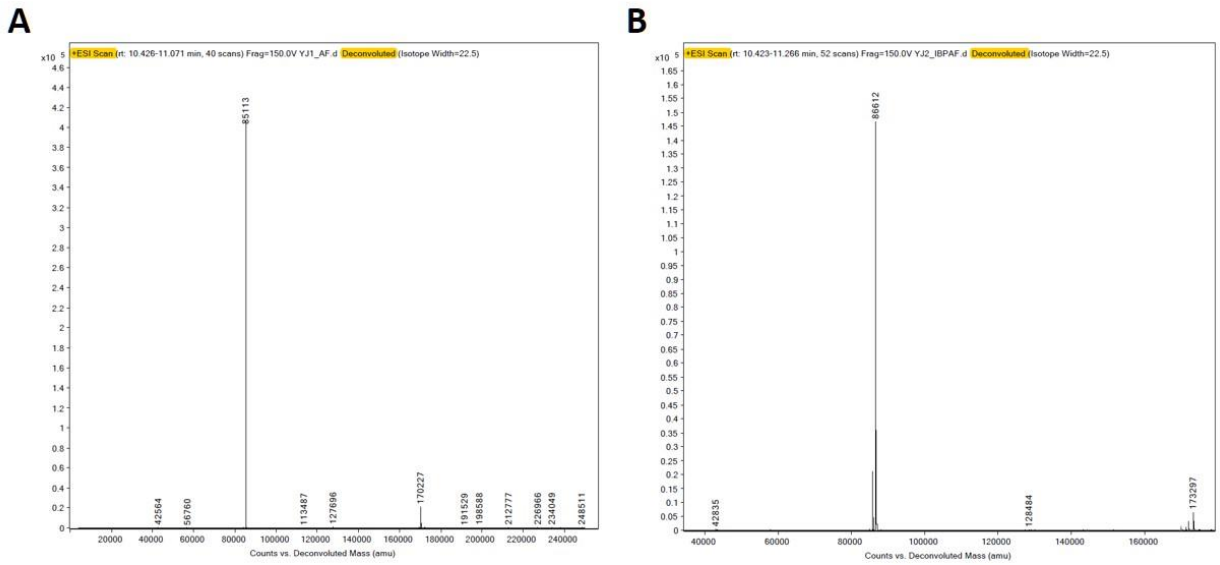

Figure S2. Molecular weights of AF and IBPAF were confirmed by electrospray ionization time-of-flight mass spectrometry. A). Counts versus Deconvoluted Mass plot of AF. B). Counts versus Deconvoluted Mass plot of IBPAF.

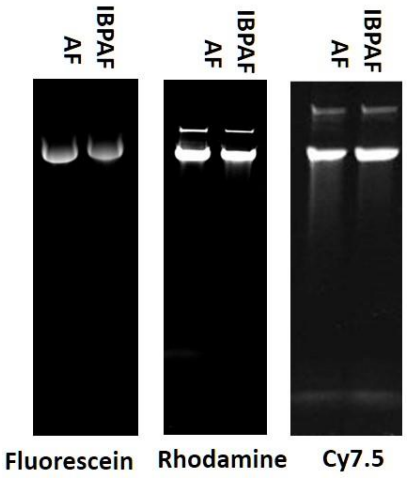

Figure S3. SDS-PAGE of fluorescently-labeled AF and IBPAF. After AF and IBPAF were labeled with NHS-Fluorescein, NHS-Rhodamine, or Sulfo-Cyanine7.5 (Cy7.5) NHS esters, SDS-PAGE was run to confirm the absence of contaminating excess dye.

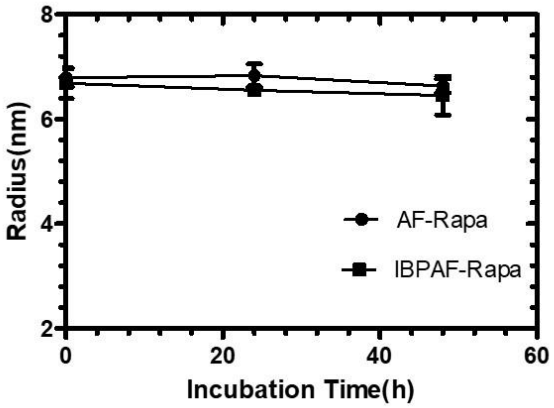

Figure S4. Hydrodynamic radii of AF-Rapa complex and IBPAF-Rapa complex versus time of incubation at 37°C. AF-Rapa and IBPAF-Rapa complexes were incubated at 37°C and the hydrodynamic radii was measured at different time points (n=3 for each time point).

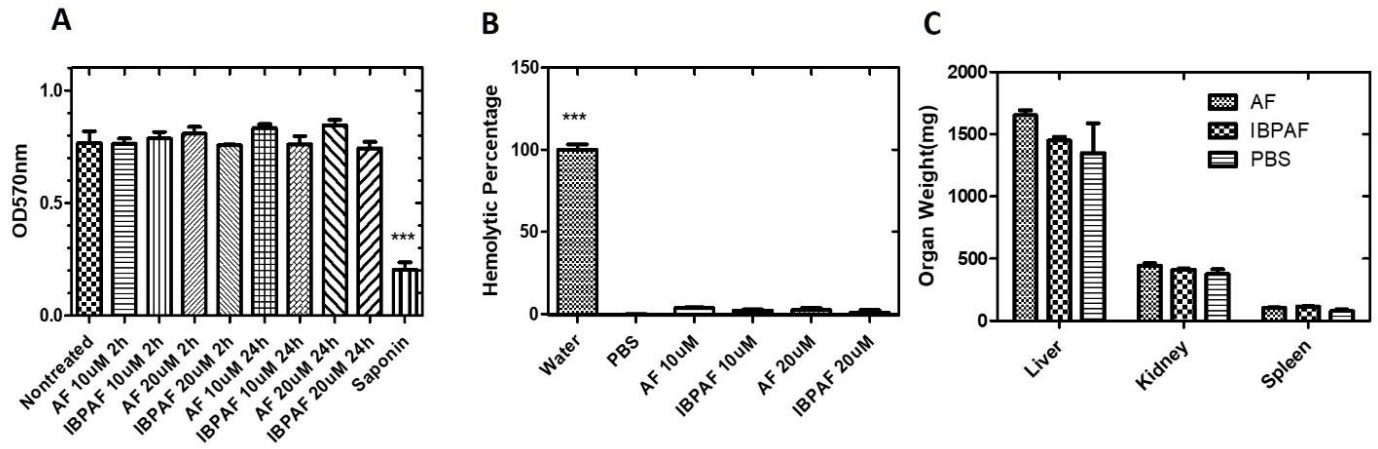

Fig S5. Cytotoxicity and biocompatibility of AF and IBPAF. A) An MTT assay was done to determine the cytotoxicity of AF and IBPAF at the indicated doses of 10 and 20 μM after 2h or 24h incubation with the mouse hepatocyte cell line 644 at 90% confluency. No significant differences were seen in any ELP treatment groups versus PBS treatment, while 0.1% saponin provided a positive control for cell death (n=3). B) A hemolytic assay was performed to test whether ELP treatments caused hemolysis of mouse red blood cells. Water was used as a positive control to promote lysis, and PBS was used as a negative control for no lysis. No significant differences were seen in any ELP treatment group versus PBS (n=3). C) Weights of liver, kidney and spleen were measured 24h after mice were injected with 150 μl of 200 μM AF, IBPAF or PBS. No significant differences were seen between AF, IBPAF and PBS (n=5 for AF and IBPAF, n=2 for PBS).

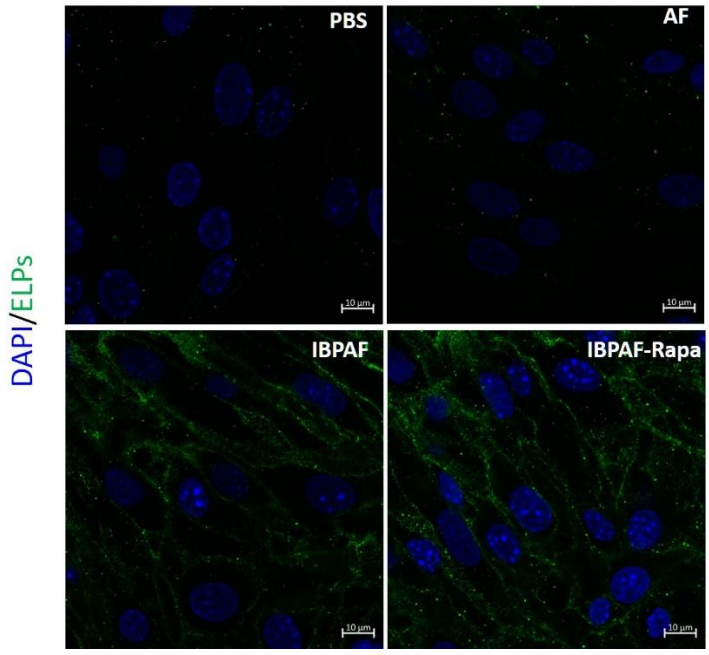

Fig S6. Binding of IBPAF-Rapa and IBPAF to cell surface ICAM-1 is comparable in bENd.3 cells. TNF-α stimulated bENd.3 cells were treated with 50 μM AF, IBPAF or IBPAF-Rapa at 4 °C for 30 min, respectively.

Then cells were processed for immunofluorescence labeling using anti-ELP antibody and an appropriate secondary antibody as described in Methods. Green: ELP, Blue: DAPI. Scale bar=10 μm. Results are representative of n=2.

Supplemental Material and Methods

ELP Purification, Biophysical Characterization and Fluorescent labeling

AF and IBPAF were purified according to standard protocols published previously[1, 2]. Fusion protein polymers were analyzed for purity by Coomassie blue SDS-PAGE gel analysis. The molecular weights of AF and IBPAF were confirmed by Electrospray ionisation time-of-flight mass spectrometry (ESI-TOF). The temperature-concentration phase diagram and hydrodynamic radius (Rh) at 37°C was determined as previously described [1, 3]. For fluorescent visualization in both in vitro and in vivo studies, AF and IBPAF were covalently modified with NHS-Fluorescein, NHS-Rhodamine, or Sulfo-Cyanine7.5 (Cy7.5) NHS esters, respectively, as previously described [4, 5].

Cytotoxicity and Hemolysis assay

The mouse hepatocyte cell line (644) was generously provided by Dr. Bangyan Stiles from University of Southern California. Cells were treated with 10 μM or 20 μM of AF or IBPAF for 2h or 24h, respectively. Complete culture media for mouse hepatocytes was used as negative control and 0.1% saponin was used as positive control. Cytotoxicity was analyzed by the CytoSelect™ Cell viability and cytotoxicity assay kit following the manufacturer's instruction.

For the hemolysis assay, mouse red blood cells were isolated using a published protocol[6]. Briefly, mouse whole blood was collected and stored in EDTA tubes. Red blood cells were isolated from whole blood by centrifugation and removal of the supernatant, followed by washing three times in PBS. Following the washes, red blood cells were diluted ten times in PBS. 100 μL of diluted blood was mixed with 400 μL AF or IBPAF to achieve final concentrations of each ELP at 10 μM and 20 μM, respectively. PBS and water were used as negative and positive controls, respectively. After 2h incubation at 37°C, the mixture was centrifuged at 5,000 rpm for 2 min and the supernatant was collected. The absorbance of the supernatant associated with release of hemoglobin through lysis was recorded at 541 nm. The hemolytic percentage (HP) was calculated using the following equation: $HP(\%)=(D_t-D_{nc})/(D_{pc}-D_{nc})*100\%$, where D_t is the absorbance of the test samples; D_{pc} and D_{nc} are the absorbances of the positive and negative controls, respectively.

Flow cytometry

TNF-α stimulated bEnd.3 cells were trypsinized into single-cell suspensions prior to incubation with Fluorescein-labeled AF, IBPAF or PBS at 4°C for 30 min with mild shaking. Cells were washed with ice-cold PBS and processed for further analysis using an LSRII Flow Cytometer (BD Biosciences, San Jose, CA).

Isothermal Titration Calorimetry

The drug binding affinity between Rapa and AF or IBPAF was evaluated by MicroCal PEAQ Isothermal Titration Calorimetry according to previously reported methods [7]. Briefly, titrations were performed at 37°C with Rapa at a concentration of 8 µM, in a volume of 280 µl in the calorimeter cell and with protein at a concentration of 100 µM in the titration syringe, while 12 injections of the protein into the drug were made. The drug and the protein were solubilized in the same buffer (1% v/v DMSO in PBS) to prevent background heat of release due to differences in buffer composition.

Real-Time PCR

Total RNA was isolated from different organs of NOD and BALB/c mice and converted to cDNA. Quantitative (real-time) PCR (qPCR) was performed with TaqMan gene expression assays using probes for ICAM-1 (Mm00516024_g1) and GAPDH (Mm99999915_g1). The relative expression levels were calculated using the comparative CT method (ΔΔCT method) as described previously [8].

Western Blotting

Whole cell lysates or tissue lysates were prepared using RIPA buffer containing protease inhibitors as previously described [9]. 40 µg of total protein was resolved on PAGEr EX 10% gradient gels and then transferred to nitrocellulose membranes. The membranes were incubated with anti-ICAM-1 and anti-actin primary antibodies, followed by secondary antibodies and imaged using a Li-Cor Odyssey Scanning Infrared Fluorescence Imaging System (Lincoln, NE).

Immunofluorescence Labeling

Mouse LG were processed as previously described [10, 11]. Briefly, LGs were fixed, embedded in O.C.T. compound and flash frozen on dry ice. Blocks were cryosectioned at 5 µm thickness and mounted on glass slides. After being quenched and permeabilized as described, tissue sections were blocked with 1% BSA followed by incubation with primary and secondary antibodies. Finally, samples were mounted with ProLong anti-fade mounting medium and imaged using a ZEISS LSM 800 confocal microscope equipped with an Airyscan detector (Zeiss, Thornwood, NY).

Liquid Chromatography–Mass Spectrometry

50ul of plasma was mixed with 50ul of 500 ng/mL Tacrolimus which served as internal control. Both Rapa and internal control was extracted by adding 500 µl Acetonitrile followed by incubation at -20 for 30 min. Supernatant was collected after spinning at 13,000rpm for 5min and dried. The pellet was reconstituted in 80% acetonitrile and further analysed by Agilent 1200 linked onto API4000. The analytes were separated using a C18 Kinetex column (Phenomenex) with the following dimension 50 ×3.0 ×2.6 µm. The mobile phase utilized a gradient system consisting of two components, where component A was water with 0.5 % formic acid and component B was acetonitrile with 0.5 % formic acid. The program consisted of 50 % Component B at time 0), where the concentration increased to 90% after two minutes and held for another five minutes. Rapa and Tacrolimus were quantified using MRM of 931.7 → 865.0 and 821.5 → 768.7, respectively.

(1) Aluri, S., Pastuszka, M. K., Moses, A. S., and MacKay, J. A. (2012) Elastin-Like Peptide Amphiphiles Form Nanofibers with Tunable Length. *Biomacromolecules 13*, 2645-2654.
(2) Meyer, D. E., and Chilkoti, A. (2002) Genetically Encoded Synthesis of Protein-Based Polymers with Precisely Specified Molecular Weight and Sequence by Recursive Directional Ligation: Examples from the Elastin-Like Polypeptide System. *Biomacromolecules 3*, 357-367.
(3) Guo, H., Lee, C., Shah, M., Janga, S. R., Edman, M. C., Klinngam, W., Hamm-Alvarez, S. F., and MacKay, J. A. (2018) A Novel Elastin-Like Polypeptide Drug Carrier for Cyclosporine a Improves Tear Flow in a Mouse Model of Sjogren's Syndrome. *J Control Release 292*, 183-195.
(4) Sreekumar, P. G., Li, Z., Wang, W., Spee, C., Hinton, D. R., Kannan, R., and MacKay, J. A. (2018) Intra-Vitreal Alphab Crystallin Fused to Elastin-Like Polypeptide Provides Neuroprotection in a Mouse Model of Age-Related Macular Degeneration. *J Control Release 283*, 94-104.
(5) Peddi, S., Pan, X., and MacKay, J. A. (2018) Intracellular Delivery of Rapamycin from Fkbp Elastin-Like Polypeptides Is Consistent with Macropinocytosis. *Front Pharmacol 9*, 1184-1184.
(6) Wang, C., Wang, S., Li, K., Ju, Y., Li, J., Zhang, Y., Li, J., Liu, X., Shi, X., and Zhao, Q. (2014) Preparation of Laponite Bioceramics for Potential Bone Tissue Engineering Applications. *Plos One 9*, e99585.
(7) Dhandhukia, J. P., Li, Z., Peddi, S., Kakan, S., Mehta, A., Tyrpak, D., Despanie, J., and MacKay, J. A. (2017) Berunda Polypeptides: Multi-Headed Fusion Proteins Promote Subcutaneous Administration of Rapamycin to Breast Cancer in Vivo. *Theranostics 7*, 3856-3872.
(8) Wu, K., Joffre, C., Li, X., MacVeigh-Aloni, M., Hom, M., Hwang, J., Ding, C., Gregoire, S., Bretillon, L., Zhong, J. F., et al. (2009) Altered Expression of Genes Functioning in Lipid Homeostasis Is Associated with Lipid Deposition in Nod Mouse Lacrimal Gland. *Exp Eye Res 89*, 319-332.
(9) Li, X., Wu, K., Edman, M., Schenke-Layland, K., MacVeigh-Aloni, M., Janga, S. R., Schulz, B., and Hamm-Alvarez, S. F. (2010) Increased Expression of Cathepsins and Obesity-Induced Proinflammatory Cytokines in Lacrimal Glands of Male Nod Mouse. *Invest Ophthalmol Vis Sci 51*, 5019-5029.
(10) Meng, Z., Edman, M. C., Hsueh, P. Y., Chen, C. Y., Klinngam, W., Tolmachova, T., Okamoto, C. T., and Hamm-Alvarez, S. F. (2016) Imbalanced Rab3d Versus Rab27 Increases Cathepsin S Secretion from Lacrimal Acini in a Mouse Model of Sjogren's Syndrome. *Am J Physiol Cell Physiol 310*, C942-954.
(11) Meng, Z., Klinngam, W., Edman, M. C., and Hamm-Alvarez, S. F. (2017) Interferon-Gamma Treatment in Vitro Elicits Some of the Changes in Cathepsin S and Antigen Presentation Characteristic of Lacrimal Glands and Corneas from the Nod Mouse Model of Sjogren's Syndrome. *Plos One 12*, e0184781.